JOURNAL OF MATERIALS SCIENCE 24 (1989) 4009–4023

An alternative model for nonlinear stress–strain behaviour of composite materials

GHAZI ABU-FARSAKH
Department of Civil Engineering, Jordan University of Science and Technology, Irbid, Jordon

An alternative model for the Jones–Nelson material model is developed, in which the secant mechanical property is assumed to be a function of the plastic strain energy density of an equivalent linear elastic system which replaces the total strain energy term in the Jones–Nelson model. The present model is capable of treating multiple mechanical property nonlinearities which are generally exhibited by fibre-reinforced composite material. The new model is represented in two forms; the basic model and the iterative model. A comparison is carried out in order to correlate strains predicted by the present model with experimental data and other theoretical models cited from the literature. What makes the new model practical is that the plastic strain energy due to loading at any fibre-orientation is not allowed to exceed the fibre direction value obtained from the uniaxial loading test. Hence, the model does not require an extension of behaviour beyond the defined range of strain energy.

1. Introduction

Most composite materials exhibit nonlinear stress–strain behaviour in at least one of the principal material directions. For example, boron/epoxy and graphite/epoxy have highly nonlinear shear behaviour. Moreover, boron/aluminium has nonlinear behaviour transverse to the fibres as well as a shear nonlinearity, and carbon/carbon has nonlinearities in all principal material directions.

The degree of nonlinearity varies from composite to composite and is due mainly to the nonlinear matrix material, which greatly affects the transverse modulus, E_2, and the shear modulus, G_{12}, of the composite. Using micromechanics analysis for normal combinitions of fibres and matrix materials [1], the effect of the nonlinear matrix material on the longitudinal modulus, E_1, and Poisson's ratio, ν_{12}, is shown to be negligible.

The nonlinearities for composite materials are more pronounced with increasing temperature and moisture content [2]. Thus, general application of composites requires analysis of nonlinear stress–strain behaviour.

Several investigators have studied the nonlinear behaviour of composite materials using different approaches. Petit and Waddoups [3] used an incremental approach to determine the stress–strain response of a lamina. Hashin *et al.* [4] used Ramberg–Osgood [5] stress–strain relations to approximate the nonlinearities. Rao and Murty [6] conceived an alternative form of the Ramberg–Osgood formula which can be directly applied to the matrix displacement method. Hahn and Tsai [7] model utilized the complementary elastic strain energy density to derive a stress–strain relation. This model considers only the nonlinearity in shear behaviour. Sandhu [8], in his incremental theory, predicted equivalent multi-axial strain increments by using an approximation of the stress–strain behaviour under biaxial normal stress states. An orthotropic material model was developed by Jones and Nelson [9–12] in which the nonlinear mechanical properties were expressed as functions of the total strain energy density. Extensions of this model were later suggested by Jones and Morgan [13]. The basic Jones–Nelson model will be discussed in the next section.

An experimental study [14] was conducted on the unidirectional carbon composites which exhibit significant hardening in longitudinal tension. Pindera and Herakovich [15] studied the nonlinear response of unidirectional graphite composites using a rational approach. An alternative constitutive equation was proposed by Ishikawa *et al.* [16], who also developed [17] an iterative procedure of the geometrical nonlinear analysis of carbon/epoxy plain-weave composites accounting for warping. It was concluded that warping contributes greatly to the apparent hardening of this composite material at low stress levels. An incremental analysis predicting the nonlinear stress–strain behaviour of laminated hybrid composites (as carbon/glass) was developed [18]. The theory accounts for the finite strain deformation and the changes of the fibre orientation angles at large deformations.

The aim of the present work was to develop a general material model capable of treating multiple mechanical property nonlinearities and to predict the stress–strain behaviour of composite materials.

2. Description of the Jones–Nelson material model

Jones and Nelson [9–12] developed an orthotropic material model in which the nonlinear mechanical properties M_i are functions of the strain energy density

$$M_i = A_i[1 - B_i(U_s/U_{0_i})^{C_i}] \quad (1)$$

0022–2461/89 $03.00 + .12

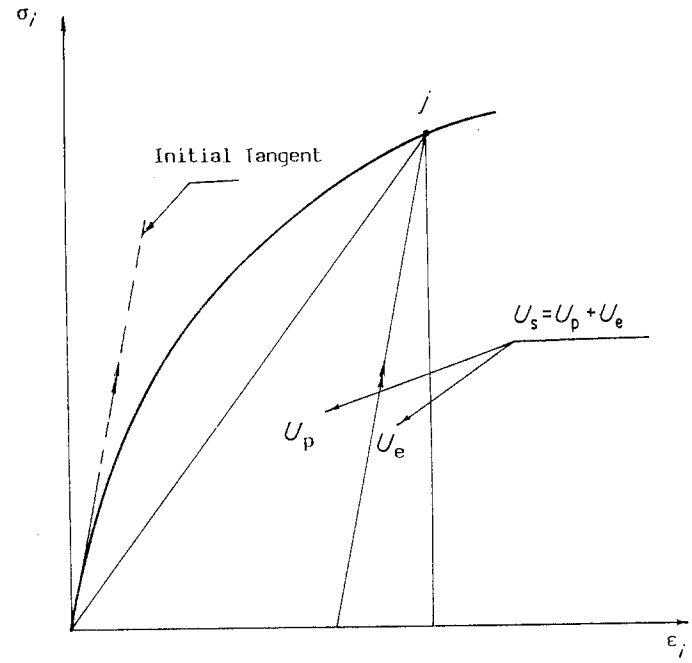

Figure 1 Typical nonlinear stress–strain curve for the ith mechanical property showing the energy terms.

where U_s is the strain energy density of an equivalent linear elastic body. The constants A_i, B_i, and C_i are the initial slope, initial curvature, and change of curvature of the ith stress–strain curve. The material property constants are determined by simultaneous solution from data at three points on the experimental curves [13]. The quantity U_0 is used to nondimensionalize the strain energy density. The Jones–Nelson model can treat multiple mechanical property nonlinearities.

The basic Jones–Nelson material model (Equation 1) is applicable only over the range in which data are defined. That is, the actual strain energy in a multiaxial stress state can exceed the defined range of mechanical property–strain energy curves. Accordingly, beyond that range, the stress–strain curve was extrapolated under the multiaxial stress state. Jones and Morgan [13] suggested different approaches to extend the basic Jones–Nelson model. In the extended model the constants A_i, B_i, and C_i were determined using nonliner regression analysis.

3. Description of the alternative model

3.1. Basic model

The basic model expresses the nonlinear mechanical property (M_i) of the ith stress–strain curve as a function of a plastic strain energy (U_p) of an equivalent linear elastic system

$$M_i = M_0[1 - B_i(\bar{U}_p)^{C_i}], \quad \bar{U}_p = U_p/U_{0_i} \quad (2)$$

where M_0 is the initial tangent value of mechanical property, B_i, C_i are the mechanical property constants of the ith stress–strain curve, U_{0_i} is used to nondimensionalize U_p (here, equals 6.89×10^{-3} N mm^{-2}).

The plastic strain-energy, U_p, is expressed as

$$U_p = U_s - U_e \quad (3)$$

where U_s is the total strain energy density of an equivalent linear elastic system, and U_e is the elastic strain energy density due to unloading.

Under the plane-stress case, the expressions for U_s and U_e are expressed for an orthotropic material as

$$U_s = \tfrac{1}{2}(\sigma_1\varepsilon_1 + \sigma_2\varepsilon_2 + \tau_{12}\gamma_{12}) \quad (4)$$

$$U_e = \tfrac{1}{2}\left(\frac{\sigma_1^2}{E_{1_0}} + \frac{\sigma_2^2}{E_{2_0}} + \frac{\tau_{12}^2}{G_{12_0}}\right) \quad (5)$$

where, 1 and 2 are the principal material directions and the symbol 0 indicates the initial tangent value of material property.

3.1.1. Determination of material property constants

The material property constants, B_i and C_i, of Equation 2 are determined by specifying two sampling data points on the ith uniaxial stress–strain curve. A least square error method is used to obtain the best curve fitting to the experimental data. The last data point on the stress–stain curve is a necessary sampling point. Solving the resulting two equations, the constants B_i and C_i are determined.

If a plot of the relation between the nondimensional value of mechanical property ($m = M_i/M_0$) against the plastic strain energy (U_p) is made, a curve will result as shown in Fig. 2. The curve intersects with the U_p-axis at U_m, where

$$U_m = \left(\frac{1}{B_i}\right)^{C_i^{-1}} \quad (6)$$

Although this model can exhibit behaviour beyond the defined range of plastic strain energy $(U_{p_i})_{max}$, nevertheless, the author believes that the U_p value at any time should not exceed that maximum value. In an explicit form this can be represented as

$$U_p \not> (U_{p_i})_{max} \quad (7)$$

for the ith mechanical property.

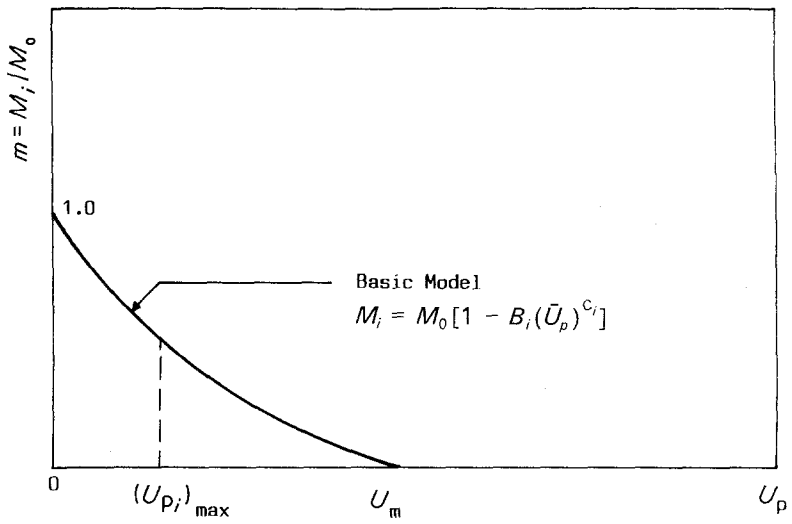

Figure 2 Shear factor–plastic strain energy behaviour for boron/epoxy and graphite/epoxy.

3.2. Iterative model

Examining the stress–strain curve of Fig. 1, it can be easily verified that

$$M_i = M_0(U_e/U_s) \tag{8}$$

Alternatively, it can be written as

$$M_i = M_0(1 - U_p/U_s) \tag{9}$$

The above relation (Equation 8 or 9) represents an exact fitting to the experimental data curve. In order to benefit from this criterion, the optimal performance of the model can be obtained by satisfying both Equations 2 and 8 (or 9) simultaneously. This can be accomplished by developing a new iteration technique to determine a new value of the elastic strain energy (U_{e_n}). At each iteration, the next value of elastic strain energy is taken as the average of the old (U_{e_o}) and new (U_{e_n}) values, see next section. The adopted convergence criterion is

$$\left|\frac{U_{e_n} - U_{e_o}}{U_{e_n}}\right| \leqslant \varepsilon \tag{10}$$

where ε is a small number, taken here to be 10^{-4}.

3.3. Computation method

3.3.1. Basic model

In the following, the general iterative procedure used to solve the resulting nonlinear strain equations at a specified stress value is described.

1. Express the nonlinear mechanical property in terms of the plastic strain energy (U_p) from the available uniaxial test data of a lamina (i.e. σ_2–ε_2 curve, τ_{12}–γ_{12} curve, etc.).
2. Specify a certain stress level and then determine the correponding elastic strain energy, U_{e_o} (Equation 5).
3. Determine the total strain energy, U_{s_o} (Equation 4), and then calculate the plastic strain energy, U_{p_o} (Equation 3).
4. Substitute the resulting value of U_{p_o} into Equation 2 to determine the ith secant mechanical property, M_i.
5. Calculate the compliances, S_{kj}, in the strain–stress relations [19], and then determine the transformed compliances, $\bar{S}_{kj}$, according to loading directions.
6. Determine the required strains.
7. Determine the new plastic strain energy U_{p_n}, where

$$U_{p_n} = U_{s_n} - U_{e_o} \tag{11}$$

8. Check the convergence criterion

$$\left|\frac{U_{p_n} - U_{p_o}}{U_{p_n}}\right| \leqslant \varepsilon \tag{12}$$

where ε is a small value, taken here to be 10^{-4}.

If the convergence criterion is not satisfied, then repeat steps 4 to 8 using the new value of plastic strain energy, U_{p_n}, instead of the old value, U_{p_o}.

9. At this stage the strains are fully determined at a specific stress level.
10. For strains to be determined at other stress levels, repeat steps 2 to 9.

3.3.2. Iterative model

The computation technique of the iterative model represents a continuation to the steps of the basic model. The steps of computation are as follows.

1. Apply steps 1 to 9 of the basic model.
2. Before applying the next stress value, determine the new values of total strain energy (U_{s_n}) and plastic strain energy (U_{p_n}).
3. Substitute the value of U_{p_n} in the mechanical property Equation 9 in order to find the corresponding M_i.
4. Obtain the new transformed compliances, $\bar{S}_{kj}$, then determine the new strains.
5. Determine the new value of total strain energy, U_{s_m}.
6. Calculate the elastic strain energy U_{e_m}, where

$$U_{e_m} = U_{s_m} - U_{p_n} \tag{13}$$

7. Check the convergence criteria

$$\left|\frac{U_{e_m} - U_{e_n}}{U_{e_m}}\right| \leqslant \varepsilon \tag{14}$$

where ε is taken to be 10^{-4}.

8. Calculate the average value of elastic strain energy $(U_e)_{ave}$ where

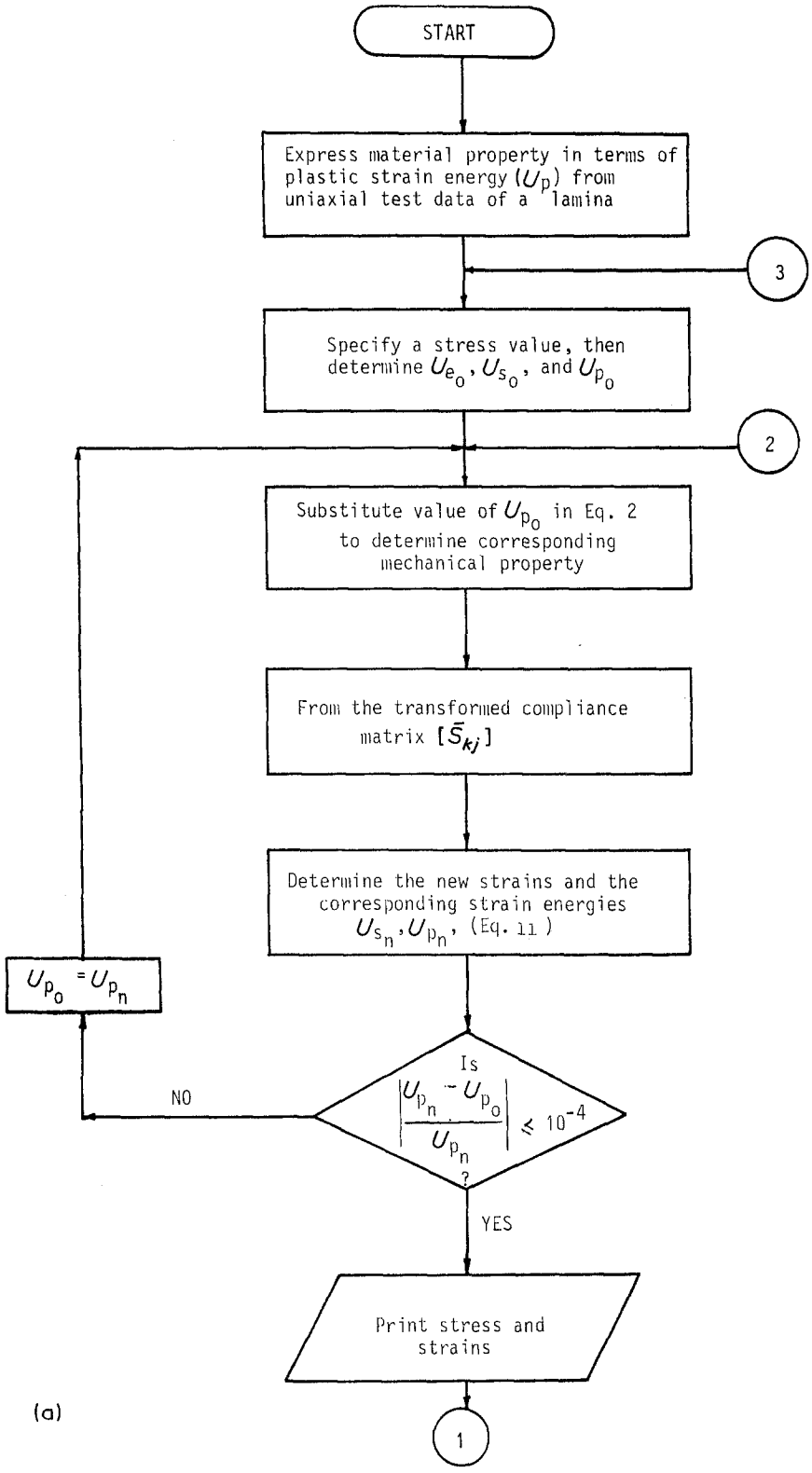

Figure 3 Flow charts for (a) the basic material model, (b) the iterative material model.

$$(U_e)_{ave} = \left(\frac{U_{e_m} + U_{e_n}}{2}\right) \quad (15)$$

It should be noted that U_{e_n} the first time is taken as U_{e_0}.

9. Determine the value of U_{p_m}, where

$$U_{p_m} = U_{s_n} - (U_e)_{ave} \quad (16)$$

If the convergence criterion is not satisfied, then move to the next step, otherwise move to step 11.

10. Repeat all previous steps until convergence criterion (Equation 14) is satisfied.

11. Determine the final strains.

12. In order to determine strains at other stress levels, repeat all previous steps.

For further clarification of the computation method, a flow chart is represented as shown in Fig. 3.

4. Uniaxial off-axis loading results

It can be easily seen from Equation 2, that the mechanical property of a composite material is determined

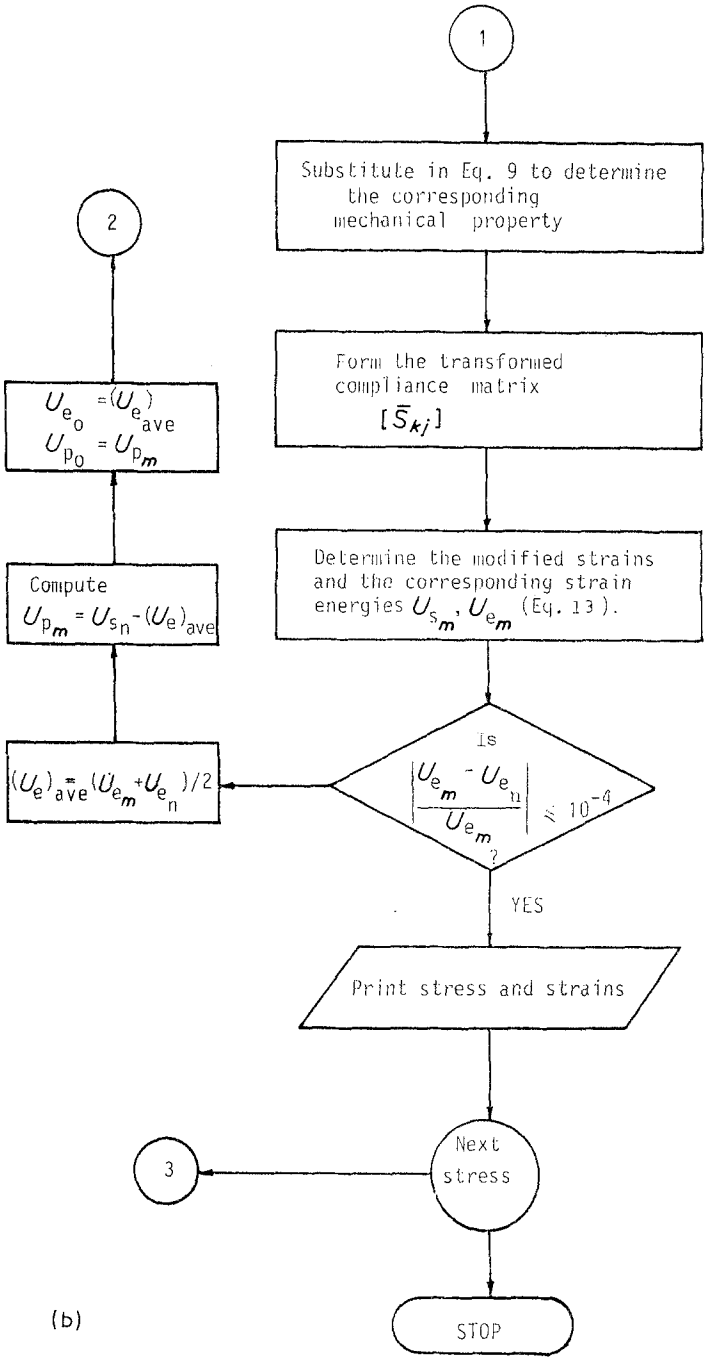

Figure 3 Continued

once the plastic strain energy, U_p, is known. However, the value of U_p is not known because the stress, strains, and mechanical properties are highly interdependent. There are several methods for solving the resulting nonlinear equations such as the numerical methods. An explicit relation for the axial strain, ε_x, in terms of the loading and known material parameters including the nonlinear shear term, was obtained by Hahn and Tsai [7]. In the present work, the iteration technique (also used in [13]) is adopted, as explained in the previous section. At convergence, the final linear elastic system is equivalent to the secant moduli of the nonlinear system. It is worth mentioning that this technique is unchanged irrespective of the number of nonlinear mechanical properties or the number of loadings. Moreover, the iteration technique is general in the sense that it can be used for an N-layered laminate. Finally, the technique can be easily incorporated in any finite element formulation.

For prediction of the strains in a lamina under uniaxial loading (in the x-direction) at some angle, θ, from the principal material 1-axis, such that

$$\sigma_x = \sigma, \sigma_y = \tau_{xy} = 0 \tag{17}$$

the strains in this case are related to the applied stress through

$$\varepsilon_x = \bar{S}_{11}\sigma, \varepsilon_y = \bar{S}_{12}\sigma, \gamma_{xy} = \bar{S}_{16}\sigma \tag{18}$$

where the $\bar{S}_{kj}$ are the transformed compliances [19] which in their turm depend on the plastic strain energy, U_p.

4.1. Results of boron/epoxy lamina

The uniaxial test data for boron/epoxy (NARMCO

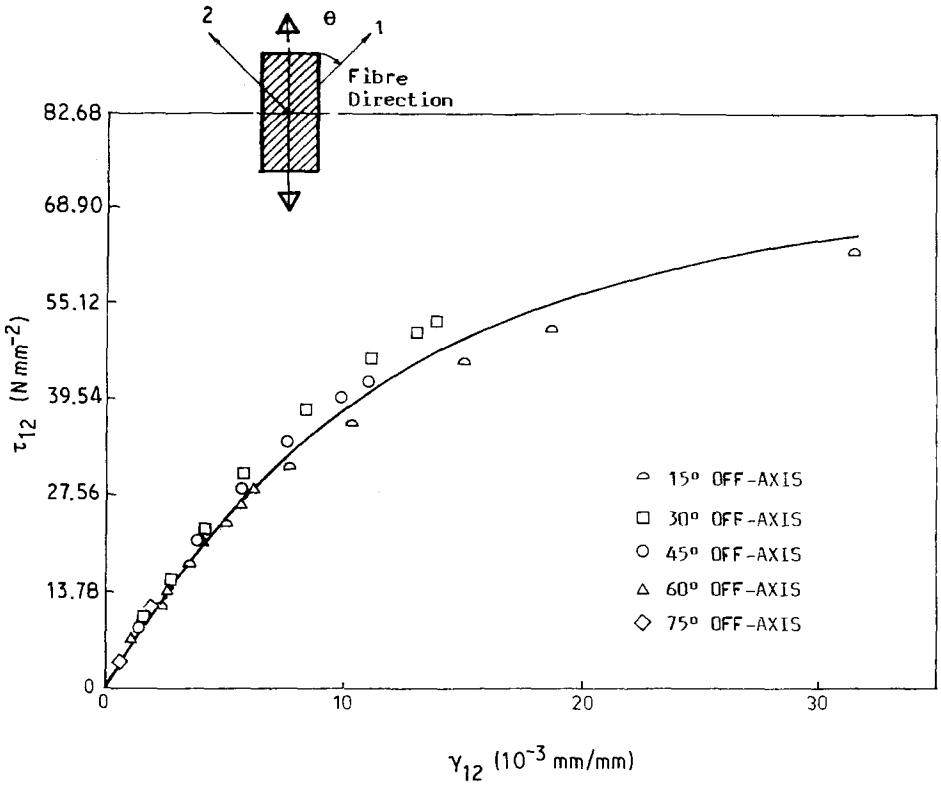

Figure 4 Boron/epoxy Narmco 5505 resolved shear behaviour. (⌓) 15°, (□) 30°, (○) 45°, (△) 60°, (◇) 70° off-axis.

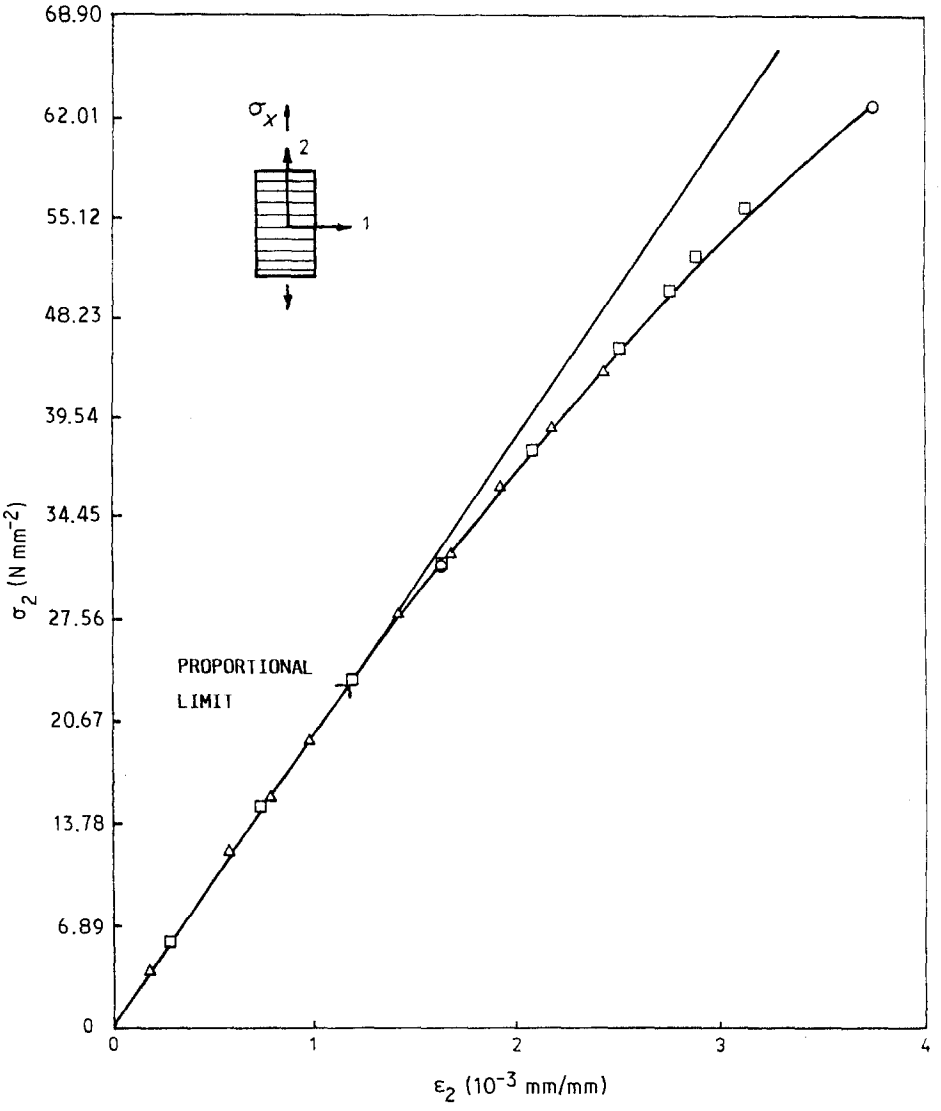

Figure 5 Boron/epoxy Narmco 5505 transverse tension stress–strain behaviour. $E_{22} = 19.77 \times 10^3$ N mm^{-2}.

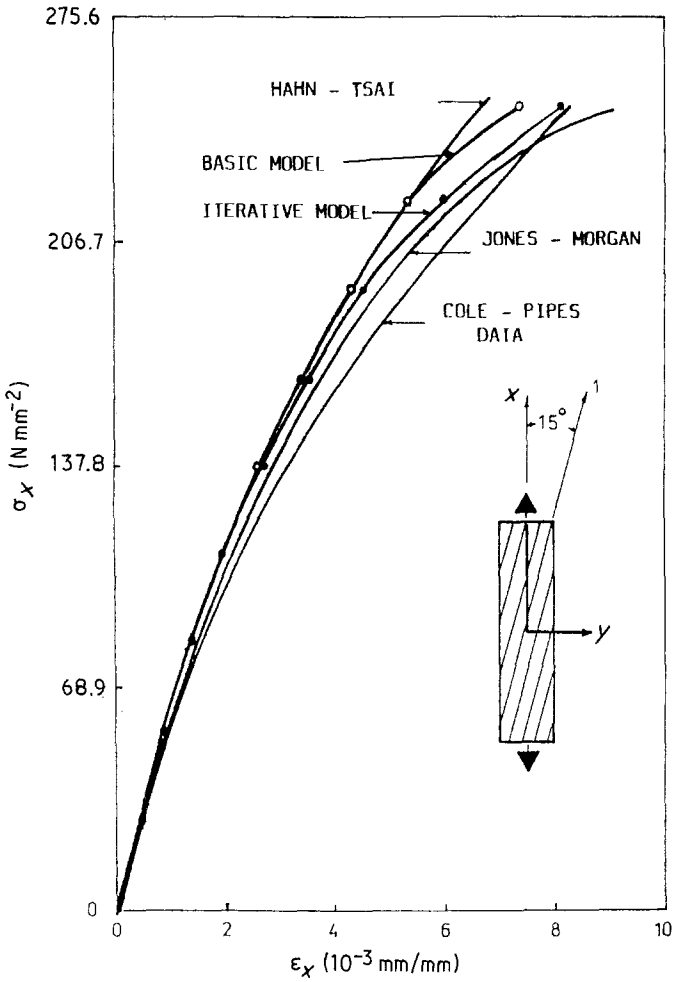

Figure 6 Boron/epoxy Narmco 5505 stress–strain behaviour (θ = 15°).

5505) were those measured by Cole and Pipes [20]. It was detected that this composite has a significant nonlinear shear behaviour (τ_{12}–γ_{12} curve or the G_{12} curve), while the curve of E_2 was slightly nonlinear. On the other hand, the curves of E_1 and ν_{12} were linear. Thus, the constant properties are

$$E_1 = 207.4 \times 10^3 \text{N mm}^{-2}, \nu_{12} = 0.225 \quad (19)$$

The nonlinear material model was developed by fitting the model (Equation 2) to the uniaxial shear stress–shear strain (τ_{12}–γ_{12}) curve due to Cole and Pipes [20]. An initial G_{12} value of 5.5 × 10^3 N mm^{-2} was considered, the same as that of Hahn and Tsai. However, a higher initial value of 6.96 × 10^3 N mm^{-2} was reported by Jones and Morgan [13]. The mechanical property constants (Table I) of boron/epoxy were obtained using a two-point least square fit to the τ_{12}–γ_{12} curve as explained earlier in this paper. Five sets of results were obtained for the predicted strains under uniaxial loading at 15°, 30°, 45°, 60° and 75° to the fibre direction, see Figs 4 to 8 inclusive.

TABLE I Material property constants for boron/epoxy from uniaxial test data of Cole and Pipes [20]

Material property	Initial mechanical property (N mm^{-2})	B_i	C_i
E_1	207.4 × 10^3	0	1
E_2	19.78 × 10^3	0.009 229	0.546 93
G_{12}	5.44 × 10^3	0.135 330	0.34016
ν_{12}	0.225	0	1

4.1.1. Results of 15° off-axis loading

The measured strains were carried out by Cole and Pipes [20] for stresses up to 248 N mm^{-2} for which the strain energy is 1.01 N mm^{-2} (U_p = 0.53 N mm^{-2}). Although the shear behaviour is known only up to a strain energy of 0.96 N mm^{-2} (see Fig. 4) where U_p = 0.64 N mm^{-2}, an extrapolation of the basic model is unnecessary because the plastic strain energy is still higher. That is, the value of plastic strain energy, U_p, of 0.53 N mm^{-2} which corresponds to the total strain energy 1.01 N mm^{-2} is still less than the U_p value of 0.64 N mm^{-2} at the total strain energy 0.96 N mm^{-2}. This also explains why a model based on the total strain energy (U_s) approach requires an extension [13], while a model based on the plastic strain energy (U_p) approach does not require an extension at higher strain energies.

Consequently, this strengthens the idea of not exceeding the maximum values of plastic strain energy, $(U_{p_i})_{max}$, obtained from uniaxial test data corresponding to different nonlinear mechanical properties. In other words, the maximum defined values of plastic strain energy for different nonlinear mechanical properties are considered an upper limit which the material cannot exceed for any fibre orientation.

The predicted axial strains using both the basic and

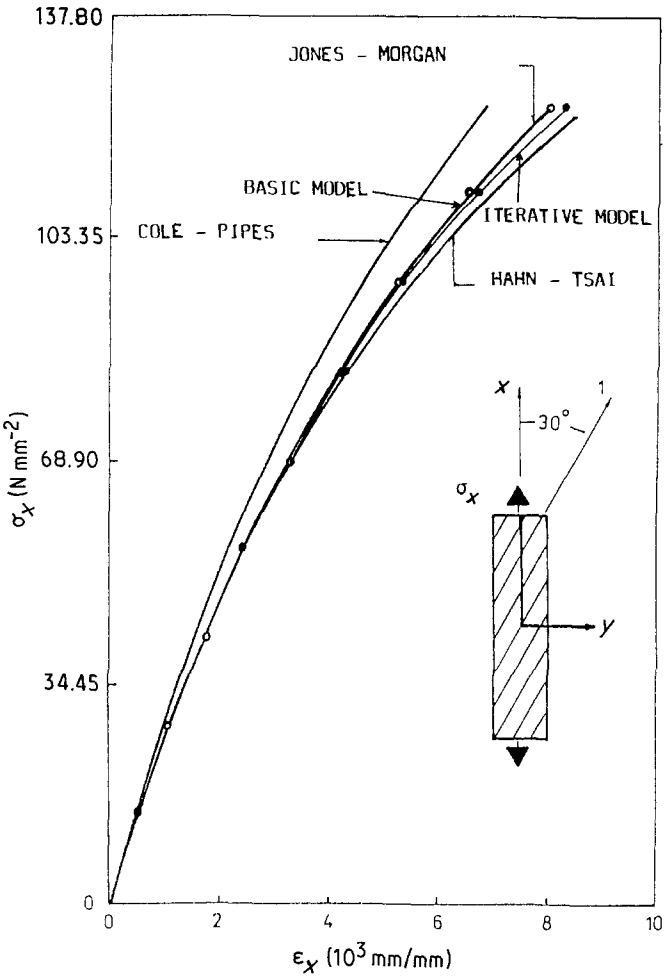

Figure 7 Boron/epoxy Narmco 5505 stress–strain behaviour (θ = 30°).

TABLE II Boron/epoxy lamina strain predictions for 15° off-axis loading (ε_x, 10^{-3} mm/mm)

σ_x (N mm^{-2})	Cole and Pipes [20] (measured)	Hahn and Tsai [7] (predicted)*	Jones and Morgan [13] (predicted)†	Present theory			
				Basic model		Iterative model	
				G_{12} nonlinearity	G_{12}, E_2 nonlinearity	G_{12} nonlinearity	G_{12}, E_2 nonlinearity
27.6	0.50	0.435	0.410	0.443	0.443	0.445	0.446
55.1	1.00	0.892	0.884	0.916	0.917	0.926	0.927
82.7	1.59	1.395	1.423	1.427	1.430	1.452	1.443
110.2	2.28	1.968	2.042	1.987	1.994	2.039	2.048
137.8	3.13	2.632	2.765	2.613	2.624	2.712	2.723
165.4	4.13	3.410	3.636	3.334	3.348	3.512	3.526
192.9	5.38	4.327	4.741	4.205	4.222	4.529	4.547
220.5	6.75	5.404	6.300	5.355	5.379	6.031	6.057
248.0	8.23	6.665	9.189	7.345	7.389	8.149	8.156

*S_{66} = 8.6 × 10^{-3} N mm^{-1} and S_{6666} = 10.54 × 10^{-11}(N mm^{-2}) [3]
†Extended τ–γ curve, slope = 430 N mm^{-2}.

TABLE III Boron/epoxy lamina strain predictions for 30° off-axis loading (ε_x, 10^{-3} mm/mm)

σ_x (N mm^{-2})	Present theory			
	Basic model		Iterative model	
	G_{12} nonlinearity	G_{12}, E_2 nonlinearity	G_{12} nonlinearity	G_{12}, E_2 nonlinearity
13.8	0.560	0.561	0.561	0.561
27.6	1.158	1.163	1.160	1.165
41.3	1.802	1.816	1.807	1.823
55.1	2.502	2.539	2.514	2.552
68.9	3.276	3.346	3.299	3.372
82.7	4.145	4.233	4.196	4.288
96.5	5.146	5.256	5.244	5.357
110.2	6.347	6.484	6.525	6.665
124.0	7.886	8.062	8.221	8.405

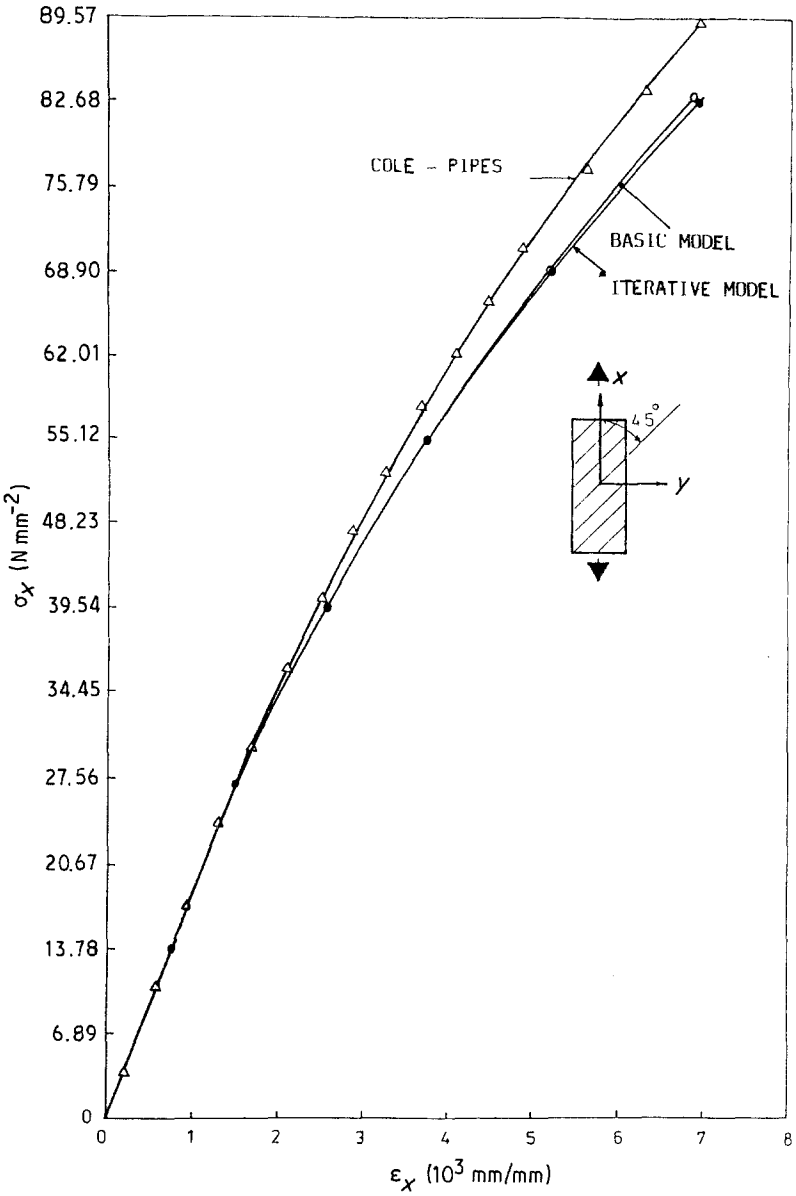

Figure 8 Boron/epoxy Narmco 5505 stress–strain behaviour ($\theta = 45°$).

TABLE IV Boron/epoxy lamina strain predictions for 45° off-axis loading (ε_x, 10^{-3} mm/mm)

σ_x (N mm^{-2})	Present theory			
	Basic model		Iterative model	
	G_{12} nonlinearity	G_{12}, E_2 nonlinearity	G_{12} nonlinearity	G_{12}, E_2 nonlinearity
13.8	0.834	0.837	0.834	0.837
27.6	1.727	1.752	1.727	1.753
41.3	2.695	2.782	2.697	2.784
55.1	3.762	3.975	3.766	3.988
68.9	4.962	5.244	5.042	5.304
82.7	6.351	6.716	6.534	6.869
96.5	8.038	8.512	8.421	8.856

TABLE V Boron/epoxy lamina strain predictions for 60° off-axis loading (ε_x, 10^{-3} mm/mm)

σ_x (N mm^{-2})	Present theory			
	Basic model		Iterative model	
	G_{12} nonlinearity	G_{12}, E_2 nonlinearity	G_{12} nonlinearity	G_{12}, E_2 nonlinearity
13.8	0.875	0.882	0.875	0.882
27.6	1.788	1.838	1.788	1.838
41.3	2.747	2.923	2.747	2.923
55.1	3.763	4.196	3.763	4.217
68.9	4.852	5.424	4.861	5.512

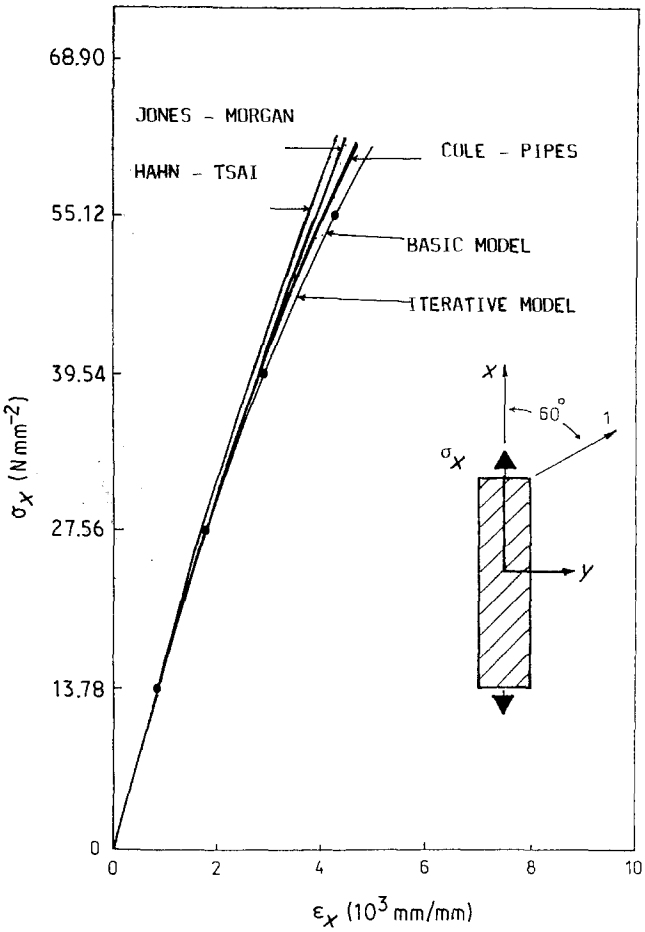

Figure 9 Boron/epoxy Narmco 5505 stress–strain behaviour (θ = 60°).

iterative models were compared to those measured by Cole and Pipes [20], Hahn and Tsai [7], and the extended Jones–Nelson model (namely Jones–Morgan material model [13]).

In Tables II to VI and Figs 6 to 10 the behaviour of the basic model is exhibited along with the iterative model (curves with E_2-nonlinearity only are shown).

By inspecting the results in Table II, it can be easily observed that the basic model predictions are approaching Hahn and Tsai's results. On the other hand, the iterative model predictions are, in general, approaching those of the Jones and Morgan model. At stress levels 220.5 N mm^{-2} and above, the iterative model predicted strains converge with those measured by Cole and Pipes.

In general, the behaviour of the iterative model is closer to the measured strains than the basic model. By referring to the results given in Table II, one can observe that strains predicted by the basic model are as low as 21.5% of the measured strains (at stress value 192.9 N mm^{-2}), while the difference is minimized to about 15.5% in the case of the iterative model. Including E_2-nonlinearity gave a slight improvement (at most 0.3%) in the predicted strains. The present strain predictions correlated well with the other models. However, if we compare the resolved initial slope, E_x, of each of the off-axis tests, we observe that the measured shear data are inconsistent (see Fig. 4). That is, we find the shear modulus, 6.89 $G_{12} \times 10^{-3}$ N mm^{-2})$^{-1}$ is equal to 0.655, 0.843, 0.871, 0.795, and 0.662 for θ = 15°, 30°, 45°, 60°, and 75°, respectively. These discrepancies are not due to shear coupling [21] because the test specimens are too long for such an influence to exist. It was found that the maximum predicted error due to shear coupling is 4% and occurs at θ = 15°, while the errors for other off-axis angles are not more than 1% [13, 20]. An explanation of such a discrepancy of shear test results may be attributed to the cure cycle where the specimens are loaded at different times in the life of the material.

TABLE VI Boron/epoxy lamina strain predictions for 75° off-axis loading (ε_x, 10^{-3} mm/mm)

σ_x (N mm^{-2})	Present theory			
	Basic model		Iterative model	
	G_{12} nonlinearity	G_{12}, E_2 nonlinearity	G_{12} nonlinearity	G_{12}, E_2 nonlinearity
13.8	0.764	0.770	0.764	0.770
27.6	1.535	1.579	1.535	1.579
41.3	2.314	2.477	2.314	2.477
55.1	3.100	3.563	3.100	3.562

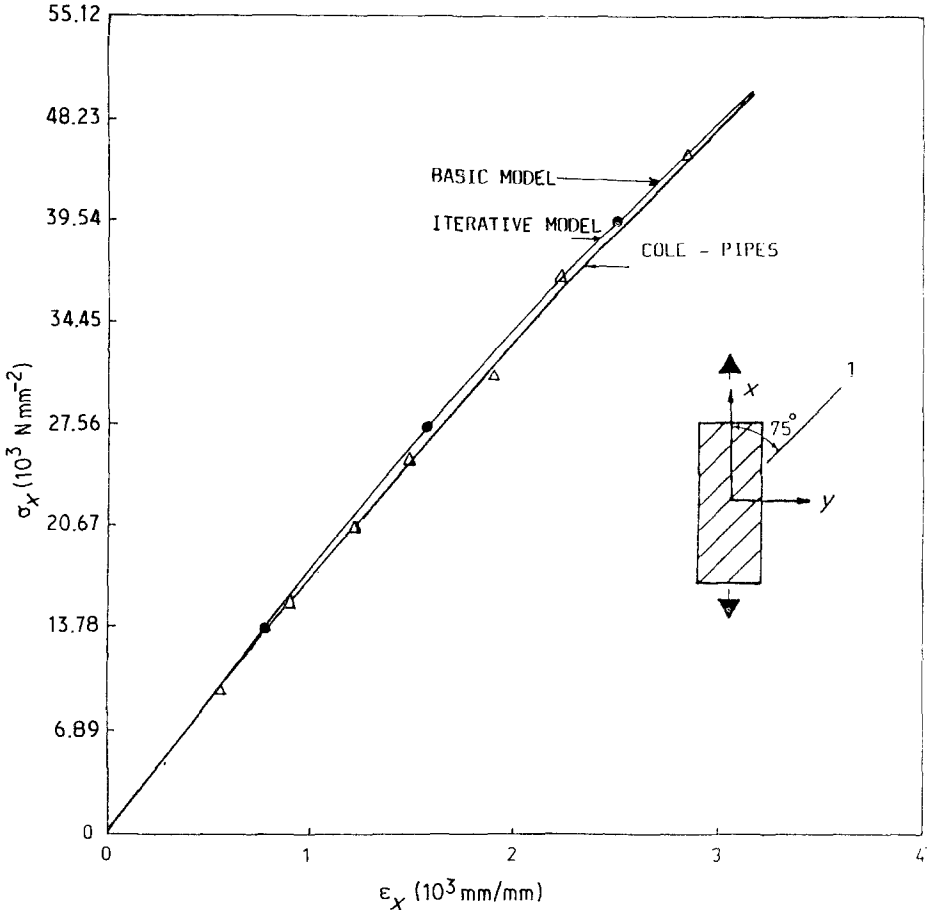

Figure 10 Boron/epoxy Narmco 5505 stress–strain behaviour ($\theta = 75°$).

4.1.2. Results of 30° off-axis loading

The basic model strain predictions are of a maximum error 14.3% of the measured results (without including E_2-nonlinearity) which occurs at 124 N mm^{-2} stress value, while that error reaches 19.2% using the iterative model (Table III). Including the E_2-nonlinearity adversely affects the results and will cause the error to increase 2.6% for the basic and iterative model. On the other hand, the Jones–Morgan and Hahn–Tsai results are 27% and 19% too high at that stress level, respectively, without including the E_2-nonlinearity effect (see Fig. 7).

4.1.3. Results of 45° off-axis loading

For 45° off-axis loading, the iterative model strain predictions (Fig. 8) are close to the measured strains. A maximum error of 11% (including E_2-nonlinearity) occurs at a stress level of 89.6 N mm^{-2} (Table IV).

4.1.4. Results of 60° off-axis loading

The iterative model strain predictions (including E_2-nonlinearity, Table V), are close to the measured strains at all stress levels, see Fig. 9, while results of the other models are lower.

4.1.5. Results of 75° off-axis loading

As shown in Fig. 10, the iterative model strain predictions are almost identical to the measured strains.

A general observation from the off-axis loading results, is that strains predicted by the iterative model are higher than those predicted by the basic model (Tables II to VI).

4.2. Results of graphite/epoxy lamina

The stress–strain response of graphite/epoxy (4617/Modmor II) is similar to that of boron/epoxy in the sense that both composite materials have considerable nonlinear shear behaviour. The mechanical property constants are given in Table VII. An initial shear

TABLE VII Material property constants for graphite/epoxy from uniaxial test data due to Cole and Pipes [20]

Material property	Initial mechanical property (N mm^{-2})	B_i	C_i
E_1	175 × 10^3	0	1
E_2	8.6 × 10^3	0	1
G_{12}	6.7 × 10^3	0.004 517	0.536 26
ν_{12}	0.46	0	1

TABLE VIII Graphite/epoxy lamina strain predictions for 15° off-axis loading (ε_x, 10^{-3} mm/mm)

σ_x (N mm^{-2})	Present theory	
	Basic model, G_{12} nonlinearity	Iterative model, G_{12} nonlinearity
34.45	0.499	0.499
68.9	1.000	1.002
103.35	1.508	1.516
137.8	2.027	2.049
172.25	2.563	2.614
206.7	3.128	3.231
241.15	3.736	3.940
275.6	4.414	4.833
310.05	5.226	5.900

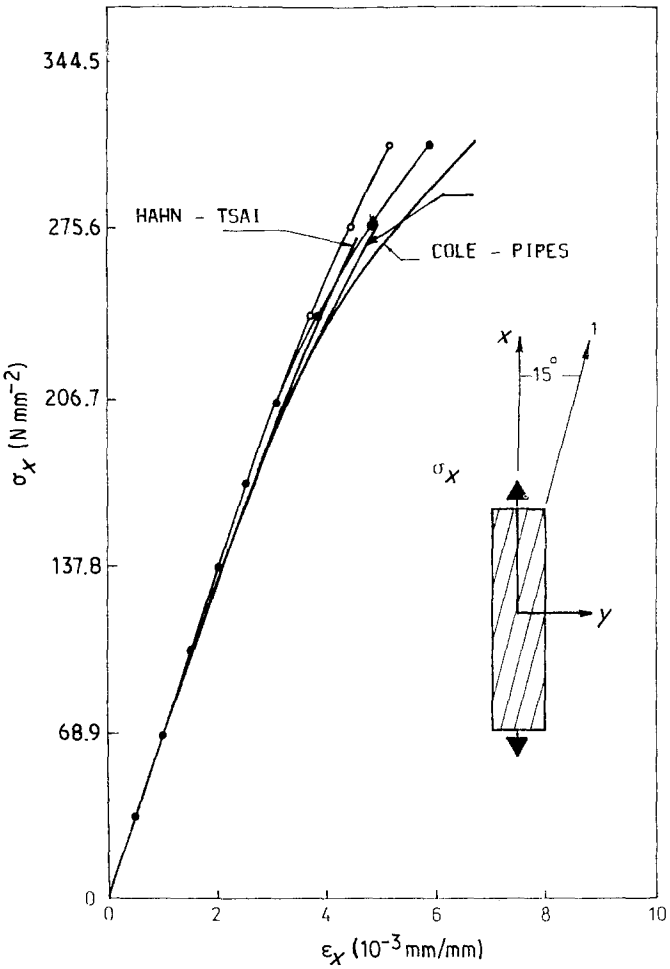

Figure 11 Graphite/epoxy 4617 Modmor II stress–strain behaviour (θ = 15°). G_{12} (elastic) = 6.72 × 10^3 N mm^{-2}.

modulus (G_0 modulus) of 6.7 × 10^3 N mm^{-2} is considered, the same as that used by Hahn and Tsai [7]. In contrast, Jones and Morgan [13] used an initial modulus of 6.23 × 10^3 N mm^{-2}.

4.2.1. Results of 15° off-axis loading

The iterative model strain predictions (Table VIII) are identical to those predicted by Hahn and Tsai up to 275.6 N mm^{-2} stress value. The Jones and Morgan results are closer to the measured strains than the present results. However, all the curves are identical over a substantial portion of the data, as shown in Fig. 11. At stress values higher than that, the iterative model results showed an improvement of behaviour which correlates well with the measured data. Results of the other models are not reported at higher stress values than 275.6 N mm^{-2}.

If we compare the resolved initial slope, E_x, of each of the off-axis tests, we observe that the measured shear data are not consistent as illustrated in Fig. 12. This inconsistency is due to reasons discussed earlier in this paper (the case of boron/epoxy lamina).

4.2.2. Results of 30° off-axis loading

The present iterative model strain predictions are almost identical with the measured strains, see Fig. 13. Results of the other models at this loading direction are not reported. The basic model strain predictions are less accurate (Table IX).

TABLE IX Graphite/epoxy lamina strain predictions for 30° off-axis loading (ε_x, 10^{-3} mm/mm)

σ_x (N mm^{-2})	Present theory	
	Basic model, G_{12} nonlinearity	Iterative model, G_{12} nonlinearity
13.78	0.516	0.515
27.56	1.032	1.033
39.54	1.552	1.554
55.12	2.078	2.084
68.9	2.611	2.625
82.68	3.156	3.183
96.46	3.717	3.764
110.24	4.300	4.378
124.02	4.911	5.037
137.8	5.562	5.760
151.58	6.269	6.582
165.36	7.059	7.570
179.14	7.984	8.899

TABLE X Graphite/epoxy lamina strain predictions for 45° off-axis loading (ε_x, 10^{-3} mm/mm)

σ_x (N mm^{-2})	Present theory	
	Basic model, G_{12} nonlinearity	Iterative model, G_{12} nonlinearity
13.78	0.915	0.915
27.56	1.832	1.834
39.54	2.755	2.765
55.12	3.688	3.716
68.9	4.637	4.699
82.68	5.609	5.730
96.46	6.613	6.835

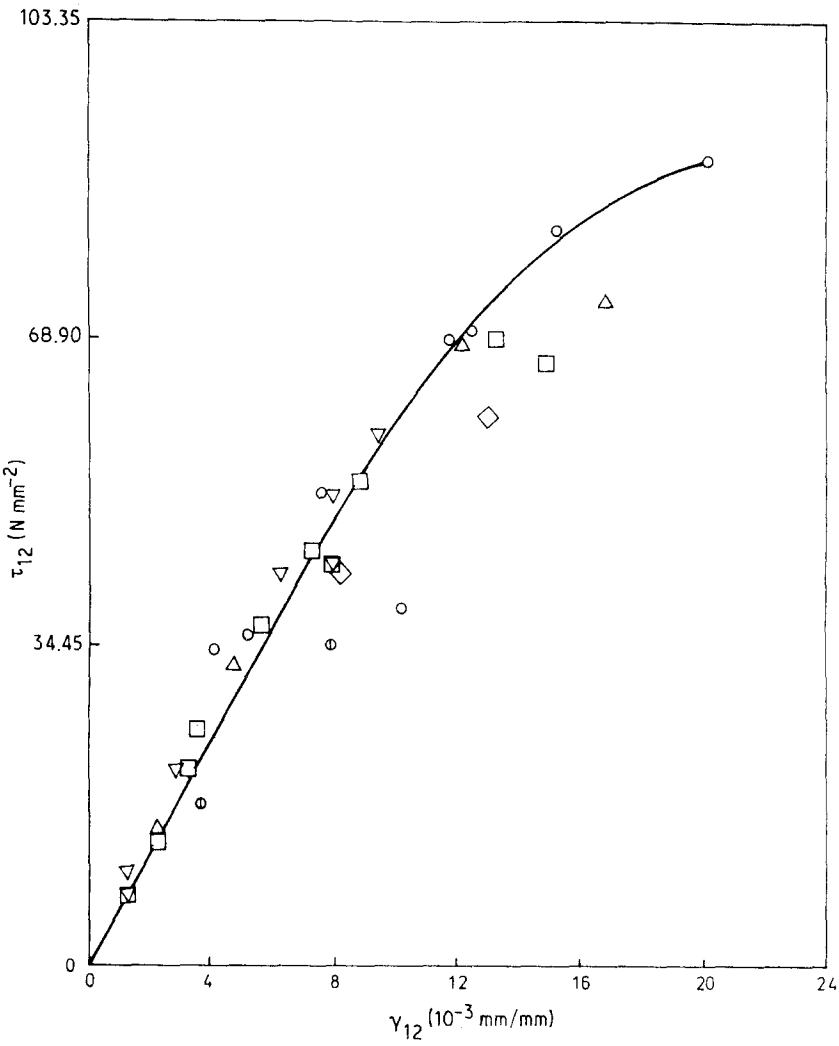

Figure 12 Graphite/epoxy 4617 Modmor II resolved lamina shear behaviour.

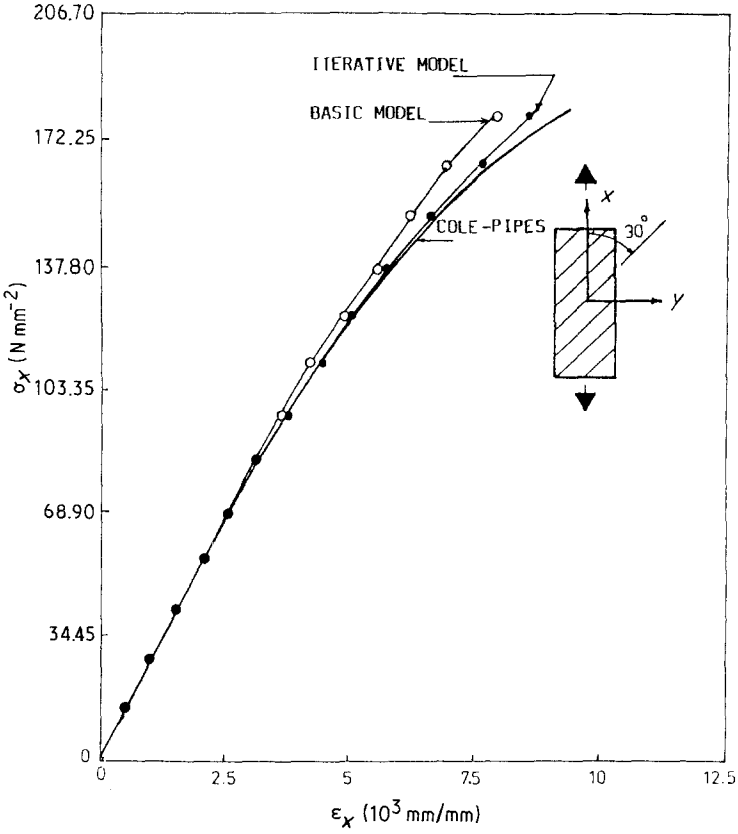

Figure 13 Graphite/epoxy 4617 Modmor II stress-strain behaviour (θ = 30°).

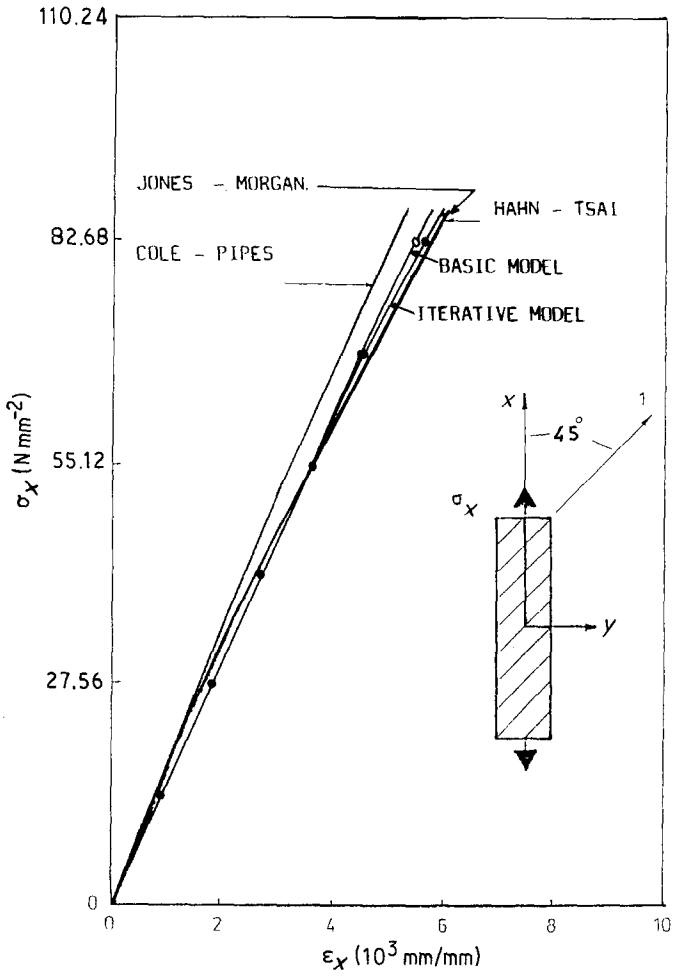

Figure 14 Graphite/epoxy 4617 Modmor II stress–strain behaviour (θ = 45°).

4.2.3. Results of 45° off-axis loading

A comparison between the present iterative model strain results is made with the other strain predictions as illustrated in Fig. 14. The behaviour of the iterative model appears to be too close to the other models over the entire range of the measured data. The basic model results are given in Table X along with the iterative model predictions.

4.2.4. Results of 60° and 50° off-axis loading

For the sake of completeness, the results of 60° and 75° off-axis loading are exhibited in Table XI and XII for both the basic and iterative models. No information of the other models, or measured data are reported in the related references.

5. Conclusions and recommendations

A new material model is described for nonlinear stress–strain behaviour of composite materials. Both the basic and iterative models can treat multiple mechanical property nonlinearities. Hence, the present model (basic or iterative) is more widely applicable than Hahn and Tsai's model with single shear nonlinearity. Moreover, it does not require an extension of behaviour at higher strain energy levels as does the Jones and Morgan extended model because of using the plastic energy term. At higher stress values, the iterative model behaviour showed a better convergence to the measured data. Although the shear data measured by Coles and Pipes were inconsistent in some cases, the predicted strains due to either model

TABLE XI Graphite/epoxy lamina strain predictions for 60° off-axis loading (ε_x, 10^{-3} mm/mm)

σ_x (N mm^{-2})	Present theory	
	Basic model, G_{12} nonlinearity	Iterative model, G_{12} nonlinearity
13.78	1.276	1.276
27.56	2.554	2.556
39.54	3.834	3.845
55.12	5.120	5.150
68.9	6.414	6.481
82.68	7.720	7.853
96.46	9.042	9.292

TABLE XII Graphite/epoxy lamina strain predictions for 75° off-axis loading (ε_x, 10^{-3} mm/mm)

σ_x (N mm^{-2})	Present theory	
	Basic model, G_{12} nonlinearity	Iterative model, G_{12} nonlinearity
13.78	1.517	1.517
27.56	3.034	3.034
39.54	4.551	4.552
55.12	6.069	6.070
68.9	7.587	7.591
82.68	9.107	9.113
96.46	10.628	10.638

were consistent. That is, the iterative model always predicts higher strains than the basic model.

The present model is applicable to general stress states, although the present study is concerned only with the uniaxial off-axis stress state. It is recommended that the present model is applied to deal with other important characteristics of composite materials. An important characteristic of many composite materials is that they exhibit different stiffnesses under compressive loading than under tensile loading (i.e. bimodulus behaviour of composite materials).

Acknowledgement

The author thanks the Deanship of Scientific Research, Jordan University of Science and Technology, for financial support of this research (grant no. 2/87).

References

1. R. M. JONES, "Mechanics of Composite Materials" (McGraw-Hill, New York, 1975).
2. J. M. WHITNEY, Air Force Workshop on Durability Characteristics of Resin Matrix Composites, Columbus, Ohio, 30 September to 2 October, 1975.
3. P. H. PETIT and M. S. WADDOUPS, *J. Compos. Mater.* **3** (1969) 2.
4. Z. HASHIN, D. BAGCHI and B. W. ROSEN, "Nonlinear Behavior of Fiber Composite Laminates", Materials Science Corp., Blue Bell, Pa., NASA CR-2313, April 1974.
5. W. RAMBERG and W. R. OSGOOD, "Description of Stress–Strain Curves by Three Parameters", NASA TN No. 902 (1943).
6. G. RAO VENKATESWARA and A. V. KRISHNA MURTY, *J. Nucl. Engng Design* **17** (1971) 297.
7. H. T. HAHN and S. W. TSAI, *J. Compos. Mater.* **7** (1973) 102.
8. R. S. SANDHU, *J. Aircraft* **13** (1976) 104.
9. R. M. JONES and D. A. R. NELSON Jr, *J. Compos. Mater.* **9** (1975) 10.
10. *Idem, ibid.* **9** (1975) 251.
11. *Idem, AIAA J.* **15** (1976) 709.
12. *Idem, ibid.* **14** (1976) 1427.
13. R. M. JONES and H. S. MORGAN, *ibid.* **15** (1977) 1669.
14. W. H. M. VAN DREVMEL and J. L. M. KAMP, *J. Compos. Mater.* **11** (1977) 461.
15. M.-J. PINDERA and C. T. HERAKOVICH, *J. Appl. Mech.* **51** (1984) 546.
16. T. ISHIKAWA and Y. HAYASHI, *J. Mater. Sci.* **20** (1985) 4075.
17. *Idem, AIAA J.* **25** (1987) 107.
18. K. TAKAHASHI and T. W. CHOU, *J. Compos. Mater.* **21** (1987) 397.
19. J. R. VINSON and T. W. CHOU, "Composite Materials and their use in structures" (Applied Science, London, 1975).
20. B. W. COLE and R. B. PIPES "Filamentary Composite Laminates Subjected to Biaxial Stress Fields", IIT Research Institute, Chicago, Illinois and Drexel University, Philadelphia, Pennsylvania, Air Force Flight Dynamics Lab. Technical Report AFFDL-TR-73-115, June, 1973.
21. N. J. PAGANO and J. C. HALPIN, *J. Compos. Mater.* **6** (1968) 18.

Received 26 February 1988
and accepted 26 January 1989